Double-threshold percolation behavior of effective kinetic coefficients

A. A. Snarskii[1,*] and M. I. Zhenirovskyy[2,†]
[1]*National Technical University of Ukraine (KPI), Kiev, Ukraine*
[2]*N. N. Bogolyubov Institute for Theoretical Physics, Kiev, Ukraine*
(Received 14 December 2007; published 11 August 2008)

We investigate thresholds of percolation in two-phase macroscopically inhomogeneous media. It is shown that, unlike standard percolation behavior there are systems in which effective kinetic coefficients of two-phase macroscopically inhomogeneous media have two percolation thresholds. As examples, thermoelectric and galvanomagnetic phenomena in such media are considered.

DOI: 10.1103/PhysRevE.78.021108 PACS number(s): 64.60.−i

INTRODUCTION

The basic characteristics of randomly inhomogeneous media are effective kinetic coefficients relating, by definition, the volume averages of thermodynamic forces and flows. Thus, for example, if we deal with a two-phase macroscopically inhomogeneous medium, wherein Ohm's law holds for each of the phases

$$\mathbf{j}(\mathbf{r}) = \sigma(\mathbf{r})\mathbf{E}(\mathbf{r}), \tag{1}$$

where $\mathbf{j}(\mathbf{r})$ and $\mathbf{E}(\mathbf{r})$ are coordinate dependences of electric current density and electric field intensity, and $\sigma(\mathbf{r})$ is local conductivity, the medium in general is characterized by the effective conductivity σ_e,

$$\langle \mathbf{j}(\mathbf{r}) \rangle = \sigma_e \langle \mathbf{E} \rangle, \tag{2}$$

where $\langle \cdots \rangle$ denotes volume averaging.

Mathematically, the effective kinetic coefficients, in this case the effective electric conductivity, are a functional,

$$\sigma_e = \sigma_e[\mathbf{j}(\mathbf{r}), \mathbf{E}(\mathbf{r})]. \tag{3}$$

Physically, this is exactly the same value that is measured experimentally, when the sample dimensions are much larger than characteristic dimensions of inhomogeneity (more precisely, more than the so-called correlation radius).

The calculation of effective kinetic coefficients has been dealt with in a large number of papers, starting with Maxwell's works (see, for example, Refs. [1–3]).

In the case of a big difference between physical properties of media, for example when the conductivity of the first phase σ_1 is much larger than that of the second phase $\sigma_1 \gg \sigma_2$, near certain concentration values of one of the two phases, the so-called percolation threshold p_c, there is a drastic change in the conductivity behavior σ_e; see Fig. 1(a). The study of such drastic changes of effective properties is a separate field of research—the so-called percolation [3].

The presence of percolation threshold p_c is due to a simple reason. With increased concentration p of phase with conductivity σ_1 ($\sigma_1 \gg \sigma_2$) at $p=p_c$, the so-called infinite-cluster continuous path in the phase with conductivity σ_1 is formed in the medium. While before the percolation threshold the current was obliged to flow through the small conducting portions with conductivity σ_2, above the threshold the major current flows in the good conducting phase, σ_1. The effective conductivity σ_e at passing through $p=p_c$ is drastically increased. Close to and at the percolation threshold itself, in the so-called critical area, the effective conductivity has a power dependence on the proximity to percola-

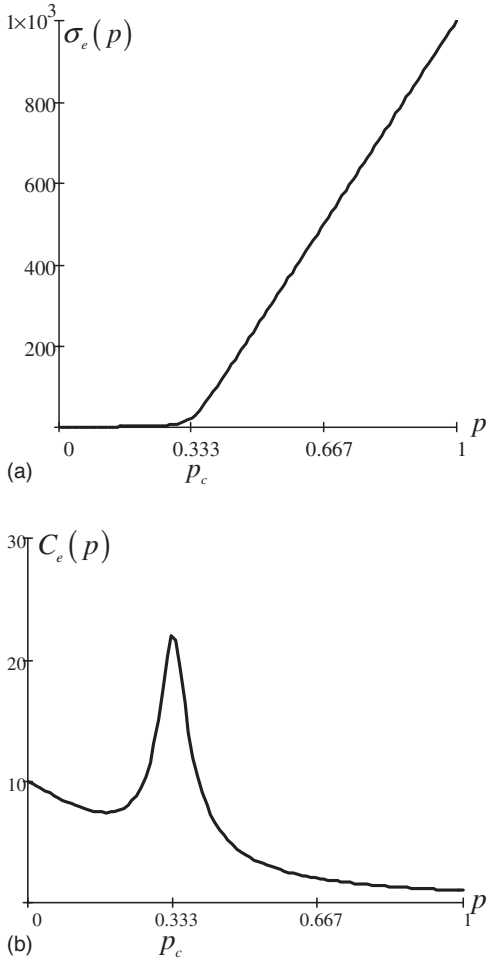

FIG. 1. Concentration behavior of effective conductivity (a) and effective spectral density of $1/f$ noise of conductivity (b) are shown. In this example, $\sigma_1=1000$, $\sigma_2=1$, $C_1=1$, and $C_2=10$; all values are in arbitrary units.

*asnarskii@gmail.com
†mzhenirovskyy@gmail.com

tion threshold $\tau=(p-p_c)/p_c$ and is characterized by universal critical exponents [1–3],

$$\sigma_e \approx \sigma_1 \tau^t, \quad p > p_c, \quad \tau > \Delta, \tag{4}$$

$$\sigma_e \approx \sigma_2 |\tau|^{-q}, \quad p < p_c, \quad |\tau| > \Delta, \tag{5}$$

$$\sigma_e \approx (\sigma_1{}^q \sigma_2{}^t)^{1/(t+q)}, \quad |\tau| \leqslant \Delta, \tag{6}$$

where $\Delta=(\sigma_2/\sigma_1)^{1/(t+q)}$ is the smearing region, the analog of the smearing region of the second-order phase transition.

Similar to the formation of an infinite cluster of good conducting phase at $p=p_c$, at $p=\tilde{p}_c=1-p_c$ (if the concentration of p is reduced from 1) an infinite cluster is formed of small conducting phase, which, however, does not affect the behavior of σ_e [Fig. 1(a)], the effective spectral density of $1/f$ noise of conductivity [Fig. 1(b)] [4,5], higher current moments, etc.

Nevertheless, in some cases there can be basically more complicated concentration behavior of effective kinetic coefficients of the two-phase media, when their drastic change takes place close to both p_c and $\tilde{p}_c$. Thermoelectric effects, when the first phase is a good conductor of current and the second one of heat, can serve one of the numerous examples of such behavior. In this case, the effective conductivity will experience percolation transition at $p=p_c$ and effective thermal conductivity in passing through $p=\tilde{p}_c$. The effective thermoelectric coefficient, determined on the one hand by conductivity (connection of current paths in a medium) and on the other hand by thermal conductivity (formation of temperature drops to create electromotive force), will "feel" both percolation thresholds [6].

The first section of this paper will consider an abstract two-flow system with "cross" effects, its partial case being, for instance, a system with thermoelectric effects. For such systems, using the isomorphism method [7,8] one can rigorously show that the effective cross coefficient has a critical behavior close to both percolation thresholds. In the second section, the results obtained are used for the system with thermoelectric effects. The third section discusses galvanomagnetic effects. In this case, calculations are made within the effective medium theory (EMT) approximation [9,10] that was generalized in [11,12]. The problem of creating a model of percolation structure of the above cases and the possibility of nonstandard behavior of effective kinetic coefficients in the case in which critical areas near p_c and $\tilde{p}_c$ intersect are discussed in the Conclusions.

I. EFFECTIVE KINETIC COEFFICIENTS IN THE ABSTRACT TWO-FLOW SYSTEM

Let us consider the case in which two thermodynamic forces $\mathbf{E}_1$ and $\mathbf{E}_2$ give rise to two thermodynamic flows $\mathbf{j}_1$ and $\mathbf{j}_2$,

$$\begin{pmatrix} \mathbf{j}_1 \\ \mathbf{j}_2 \end{pmatrix} = \hat{S}(\mathbf{r}) \begin{pmatrix} \mathbf{E}_1 \\ \mathbf{E}_2 \end{pmatrix},$$

$$\mathbf{j}_1 = S_{11}(\mathbf{r})\mathbf{E}_1 + S_{12}(\mathbf{r})\mathbf{E}_2,$$

$$\mathbf{j}_2 = S_{12}(\mathbf{r})\mathbf{E}_1 + S_{22}(\mathbf{r})\mathbf{E}_2, \tag{7}$$

where $S_{ij}(\mathbf{r})$ are local kinetic coefficients assuming in the first and second phases the values

$$\hat{S}(\mathbf{r}) = \hat{a} = \begin{pmatrix} a_{11} & a_{12} \\ a_{12} & a_{22} \end{pmatrix} \quad \text{for the first phase}, \tag{8}$$

$$\hat{S}(\mathbf{r}) = \hat{b} = \begin{pmatrix} b_{11} & b_{12} \\ b_{12} & b_{22} \end{pmatrix} \quad \text{for the second phase}, \tag{9}$$

and, since a stationary case is considered, then

$$\mathrm{div}(\mathbf{j}_{1,2}) = 0, \quad \mathrm{rot}(\mathbf{E}_{1,2}) = 0. \tag{10}$$

The effective kinetic coefficients of system (7) are determined in a similar way [Eqs. (1) and (2)],

$$\langle \mathbf{j}_1 \rangle = S^e_{11} \langle \mathbf{E}_1 \rangle + S^e_{12} \langle \mathbf{E}_2 \rangle,$$

$$\langle \mathbf{j}_2 \rangle = S^e_{12} \langle \mathbf{E}_1 \rangle + S^e_{22} \langle \mathbf{E}_2 \rangle. \tag{11}$$

As is known [7,8,13], there is no need to solve a separate problem to determine the concentration dependences S^e_{ik}. For their determination, it is sufficient to know the concentration behavior of kinetic coefficients of the one-flow system, for example, for Eq. (1). Of course, the geometric structure of the medium (arrangement of phases) should be identical. The problem of calculating S^e_{ik} is reduced to the problem of calculating σ_e.

We will use here the most general method of reducing one problem to another [8], whereby $\hat{S}_e$ can be written as

$$\hat{S}_e = \frac{(\mu\hat{a} - \hat{b}) f(p,\lambda) + (\hat{b} - \lambda\hat{a}) f(p,\mu)}{\mu - \lambda}, \tag{12}$$

where $f(p,\lambda)$ and $f(p,\mu)$ are found from the one-flow problem,

$$\sigma_e = \sigma_1 f(p,h), \quad h = \frac{\sigma_2}{\sigma_1} \ll 1, \tag{13}$$

and in $f(p,h)$ it is necessary to replace h by the parameters λ and μ, which are the roots of a square equation,

$$(\xi a_{11} - b_{11})(\xi a_{22} - b_{22}) - (\xi a_{12} - b_{12})^2 = 0, \tag{14}$$

where one of the roots is $\xi_1=\lambda$ and the second is $\xi_2=\mu$.

We will consider the cases

$$\frac{b_{11}}{a_{11}} \ll 1, \tag{15}$$

in which the ratio between the second and first phase "conductivities" is much less than unity ("σ_2/σ_1" $\ll 1$),

$$\frac{b_{22}}{a_{22}} \gg 1, \tag{16}$$

in which the ratio between the second and first phase "thermal conductivities" is much greater than unity ("κ_2/κ_1" $\gg 1$), and

$$\frac{b_{12}}{a_{12}} \gg 1. \tag{17}$$

From Eq. (14) with regard to Eqs. (15)–(17) it follows that

$$\lambda \approx \frac{b_{11}}{a_{11}}\left(1 - \frac{b_{12}^2}{b_{11}b_{22}}\right) = \frac{\det(\hat{b})}{a_{11}b_{22}} \ll 1, \tag{18}$$

$$\mu \approx \frac{b_{22}}{a_{22}}\left(1 - \frac{a_{12}^2}{a_{11}a_{22}}\right) = \frac{a_{11}b_{22}}{\det(\hat{a})} \gg 1. \tag{19}$$

Taking this into account, Eq. (12) can be approximately written as

$$\hat{S}_e = \left(\hat{a} - \frac{\hat{b}}{\mu}\right) f(p,\lambda) + \left(\frac{\hat{b}}{\mu} - \frac{\lambda}{\mu}\hat{a}\right) f(p,\mu), \tag{20}$$

from which for the effective coefficients S_{ik}^e we get

$$S_{11}^e \approx a_{11} f(p,\lambda) + a_{22}\frac{b_{12}^2}{b_{22}^2}\tilde{a} f(p,\mu), \tag{21}$$

$$S_{22}^e \approx \frac{a_{12}^2}{a_{11}} f(p,\lambda) + a_{22}\tilde{a} f(p,\mu), \tag{22}$$

$$S_{12}^e \approx \left(a_{12} - \frac{b_{12}a_{22}}{b_{22}}\right) f(p,\lambda) + \frac{a_{22}}{b_{22}} b_{12}\tilde{a} f(p,\mu), \tag{23}$$

where notations are introduced as follows:

$$\tilde{a} = \frac{\det(\hat{a})}{a_{11}a_{22}}, \quad \tilde{b} = \frac{\det(\hat{b})}{b_{11}b_{22}}. \tag{24}$$

To obtain the concentration dependence of S_{ik}^e, it is necessary to apply to a concrete one-flow problem. In a strongly inhomogeneous medium, where inequalities (15)–(17) hold, two different cases are possible.

In the first case, in which $h \ll 1$, the local coefficient σ_1 (for simplicity it will be called the first-phase conductivity) is much greater than the local coefficient in the second phase, σ_2. Note that one should not confuse conductivity in the one-flow system and conductivity S_{11} in the two-flow system. Thus, at $\sigma_1 \gg \sigma_2$ (one-flow system), the critical area with percolation behavior is close to p_c, i.e.,

$$f(p,x)|_{x=h\ll 1} = f(p,h), \quad p \approx p_c, \tag{25}$$

and [see Eqs. (4)–(6)]

$$f(p,h) = \begin{cases} \tau^t, & \tau > 0, \quad A, \\ h|\tau|^{-q}, & \tau < 0, \quad B, \\ h^{t/(t+q)}, & |\tau| \leqslant \Delta, \quad C, \end{cases} \tag{26–28}$$

where $\tau = (p - p_c)/p_c$ and $\Delta = h^{1/(t+q)}$. In so doing, in the area close to $\tilde{p}_c$, the percolation dependences do not "work," and to determine, for instance, the behavior of $f(p \approx \tilde{p}_c, h)$, one can use the effective medium theory (EMT) approximation [9,10].

In the second case, when $h \gg 1$, percolation dependences take place close to $\tilde{p}_c$, and instead of Eqs. (4)–(6),

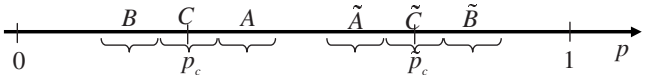

FIG. 2. The schematic image of areas corresponding to expressions (26)–(28) and (30)–(32) is shown.

$$f(p,x)|_{x=h\gg 1} = f(p,h), \quad p \approx \tilde{p}_c, \tag{29}$$

$$f(p,h) = \begin{cases} h\tilde{\tau}^t, & \tilde{\tau} > 0, \quad \tilde{A}, \\ |\tilde{\tau}|^{-q}, & \tilde{\tau} < 0, \quad \tilde{B}, \\ h^{q/(t+q)}, & |\tilde{\tau}| \leqslant \tilde{\Delta}, \quad \tilde{C}, \end{cases} \tag{30–32}$$

where now $\tilde{\tau} = (\tilde{p}_c - p)/\tilde{p}_c$ and $\tilde{\Delta} = h^{1/(t+q)}$. In so doing, close to p_c, the function $f(p \approx p_c, h)$ is determined by means of the EMT approximation.

The function $f(p,h)$ in the EMT approximation for a three-dimensional case is of the form [9,10,1,2]

$$f(p,h) = \frac{1}{4}\{3p(1-h) + 2h - 1 + \sqrt{[3p(1-h) + 2h - 1]^2 + 8h}\}. \tag{33}$$

For the case $h \ll 1$, when Eq. (33) is expanded into Taylor series in h, it can be written to a good accuracy as

$$f(p,h) = \begin{cases} \dfrac{h}{1-3p}, & p < p_c, \quad (34) \\ \dfrac{3p-1}{2}, & p > p_c. \quad (35) \end{cases}$$

For the case $h \gg 1$, when Eq. (33) is expanded into Taylor series in $1/h$,

$$f(p,h) = \begin{cases} \dfrac{3p-2}{2}, & p < \tilde{p}_c, \quad (36) \\ \dfrac{1}{3p-2}, & p > \tilde{p}_c. \quad (37) \end{cases}$$

Substituting, respectively, the values $f(p,\lambda)$ and $f(p,\mu)$ into Eq. (20), with regard to Eqs. (18) and (19), from Eqs. (26)–(32) and (34)–(37) one can determine S_{ik}^e in all the areas $A, B, \ldots, \tilde{C}$ (Fig. 2). In the A, B, C areas, $p \approx p_c$; as $\lambda \ll 1$, for $f(p,\lambda)$ it is necessary to use Eqs. (26)–(28); and as $\mu \gg 1$, for $f(p,\mu)$, the relationships (36) and (37) should be used. It is similar for the $\tilde{A}$, $\tilde{B}$, $\tilde{C}$ areas. Substituting $f(p,\lambda)$ and $f(p,\mu)$ into Eqs. (21)–(23) yields kinetic coefficients. In each of the areas, they will look as follows:

For area A,

$$S_{11}^e \approx a_{11}\tau^t, \tag{38}$$

$$S_{12}^e \approx b_{12}, \tag{39}$$

$$S_{22}^e \approx b_{22}. \tag{40}$$

For area B,

$$S_{11}^e \approx b_{11}\tilde{b}|\tau|^{-q}, \tag{41}$$

$$S_{12}^e \approx b_{12}, \tag{42}$$

$$S_{22}^e \approx b_{22}. \tag{43}$$

For area C (smearing area),

$$S_{11}^e \approx a_{11}^{q/(t+q)}(b_{11}\tilde{b})^{t/(t+q)}, \tag{44}$$

$$S_{12}^e \approx b_{12}, \tag{45}$$

$$S_{22}^e \approx b_{22}, \tag{46}$$

where in all the areas A, B, and C the effective coefficients S_{22}^e, S_{12}^e that do not experience a percolation transition were obtained in the EMT approximation, so it is not surprising that their values are almost the same in all the areas.

Let us now pass to the areas close to $\tilde{p}_c$. For area $\tilde{A}$,

$$S_{11}^e \approx a_{11}, \tag{47}$$

$$S_{12}^e \approx b_{12}\tilde{\tau}^t, \tag{48}$$

$$S_{22}^e \approx b_{22}\tilde{\tau}^t. \tag{49}$$

For area $\tilde{B}$,

$$S_{11}^e \approx a_{11}, \tag{50}$$

$$S_{12}^e \approx \frac{b_{12}a_{22}}{b_{22}}\tilde{a}|\tilde{\tau}|^{-q}, \tag{51}$$

$$S_{22}^e \approx a_{22}\tilde{a}|\tilde{\tau}|^{-q}. \tag{52}$$

For area $\tilde{C}$ (smearing area close to $\tilde{p}_c$),

$$S_{11}^e \approx a_{11}, \tag{53}$$

$$S_{12}^e \approx b_{12}(a_{22}^t\tilde{a}^t b_{22}^{-t})^{1/(t+q)}, \tag{54}$$

$$S_{22}^e \approx (a_{22}^t\tilde{a}^t b_{22}^q)^{1/(t+q)}. \tag{55}$$

Close to $\tilde{p}_c$, the effective coefficient S_{11}^e does not experience a percolation transition, and, similarly to S_{22}^e and S_{12}^e in the areas A, B, C, it is calculated in the EMT approximation.

Unlike the effective "diagonal" coefficients S_{11}^e, S_{12}^e, and S_{22}^e, each of which experiences a percolation transition close to its "own" percolation threshold, the coefficient S_{12}^e/S_{11}^e, which is responsible for cross effects, can have percolation behavior close to p_c as well as close to $\tilde{p}_c$.

For area A (see Fig. 2) from Eqs. (38) and (39) with regard to Eq. (55) we obtain

$$\frac{S_{12}^e}{S_{11}^e} = \frac{b_{12}}{a_{11}}\tau^{-t}. \tag{56}$$

For area B,

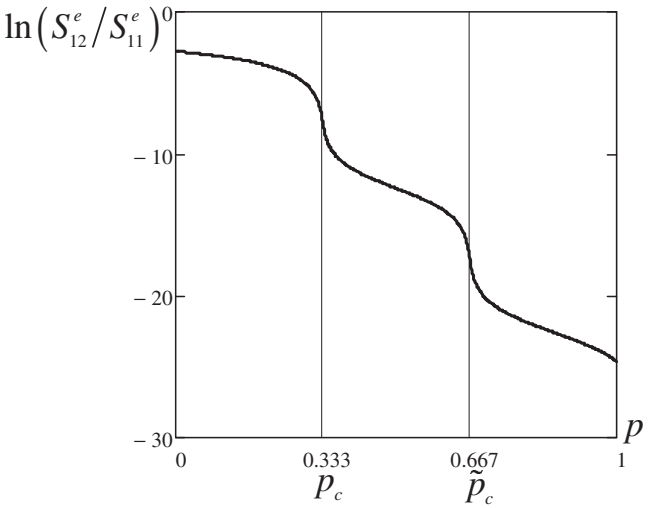

FIG. 3. Concentration behavior of the effective cross coefficient S_{12}^e/S_{11}^e close to both percolation thresholds (p_c and $\tilde{p}_c$) is shown. In this example, $A=\left(\begin{smallmatrix}5\times10^8 & 0.01\\ 0.01 & 9\times10^{-3}\end{smallmatrix}\right)$ arb. units, $B=\left(\begin{smallmatrix}3.2\times10^4 & 2000\\ 2000 & 320\end{smallmatrix}\right)$ arb. units.

$$\frac{S_{12}^e}{S_{11}^e} = \frac{b_{12}}{b_{11}\tilde{b}}|\tau|^q. \tag{57}$$

For area $\tilde{A}$,

$$\frac{S_{12}^e}{S_{11}^e} = \frac{b_{12}}{a_{11}}\tilde{\tau}^t. \tag{58}$$

For area $\tilde{B}$

$$\frac{S_{12}^e}{S_{11}^e} = \frac{b_{12}a_{22}}{a_{11}b_{22}}|\tau|^{-q}. \tag{59}$$

Figure 3 demonstrates well a drastic change in the concentration behavior of the effective cross coefficient S_{12}^e/S_{11}^e close to both percolation thresholds.

II. EFFECTIVE THERMOELECTRIC COEFFICIENTS

Knowing the effective kinetic coefficients of the abstract system, we can get them immediately for the thermoelectric case. Now instead of Eq. (7) we have

$$\mathbf{j} = \sigma\mathbf{E} + \sigma\alpha(-\nabla T),$$

$$\mathbf{\Sigma} = \sigma\alpha\mathbf{E} + \frac{\kappa}{T}(1+ZT)(-\nabla T), \tag{60}$$

where σ is electric conductivity, κ is thermal conductivity, α is thermoelectric coefficient, $Z=\sigma\alpha^2/\kappa$ is figure of merit, $\mathbf{E}$ is electric field intensity, ∇T is a temperature gradient, $\mathbf{j}$ is electric current density, and $\mathbf{\Sigma}=\mathbf{q}/T$ is entropy flow density. Effective coefficients, in conformity with Eq. (2), relate volume averages $\langle\mathbf{j}\rangle$, $\langle\mathbf{\Sigma}\rangle$, $\langle\mathbf{E}\rangle$, and ∇T,

$$\langle\mathbf{j}\rangle = \sigma_e\langle\mathbf{E}\rangle + \sigma_e\alpha_e\langle-\nabla T\rangle,$$

$$\langle \mathbf{\Sigma} \rangle = \sigma_e \alpha_e \langle \mathbf{E} \rangle + \frac{\kappa_e}{T}(1 + Z_e T)\langle -\nabla T \rangle. \tag{61}$$

Moreover, the behavior of the effective thermoelectric coefficient is directly determined as $\alpha_e \to S_{12}^e / S_{11}^e$, with the respective replacement of local coefficients. For low ZT, in agreement with Eqs. (8) and (9), we get

$$\hat{S}_i(\mathbf{r}) = \begin{pmatrix} \sigma_i & \sigma_i \alpha_i \\ \sigma_i \alpha_i & \dfrac{\kappa_i}{T} \end{pmatrix}, \quad \hat{S}_e(\mathbf{r}) = \begin{pmatrix} \sigma_e & \sigma_e \alpha_e \\ \sigma_e \alpha_e & \dfrac{\kappa_e}{T} \end{pmatrix}, \tag{62}$$

where $i=1,2$ is the phase number. From Eqs. (56)–(59) with regard to Eq. (62) for area A, we get

$$\alpha_e = \frac{\sigma_2 \alpha_2}{\sigma_1} \tau^{-t}. \tag{63}$$

For area B,

$$\alpha_e = \alpha_1 \left(1 - \frac{\sigma_2 \alpha_2 \kappa_1}{\sigma_1 \alpha_1 \kappa_2} \right) + \alpha_2 |\tau|^q. \tag{64}$$

For area $\tilde{A}$,

$$\alpha_e = \alpha_1 \left(1 - \frac{\sigma_2 \alpha_2 \kappa_1}{\sigma_1 \alpha_1 \kappa_2} \right) + \frac{\sigma_2 \alpha_2}{\sigma_1} \tau^t. \tag{65}$$

For area $\tilde{B}$,

$$\alpha_e = \frac{\sigma_2 \alpha_2 \kappa_1}{\sigma_1 \kappa_1} |\tau|^{-q}. \tag{66}$$

Thus, as can be seen from Eqs. (63)–(66), the effective thermoelectric coefficient can have critical behavior close to two percolation thresholds at the same time; see Fig. 3. Note that such behavior is possible on meeting rather "constraining" conditions for local kinetic coefficients of phases that follow from Eqs. (15)–(17). Rewriting the latter in terms of thermoelectricity yields

$$\frac{\sigma_2}{\sigma_1} \ll 1, \tag{67}$$

$$\frac{\kappa_2}{\kappa_1} \gg 1, \tag{68}$$

$$\frac{\sigma_1 \alpha_1}{\sigma_2 \alpha_2} \ll 1. \tag{69}$$

Unfortunately, for known materials, conditions (67) and (68) are incompatible. As a rule, the larger the electric conductivity of a material, the larger is its thermal conductivity (note that this fact accounts for the low figure of merit and, eventually, the low efficiency of thermoelectric devices). This empirical rule, with the Wiedemann-Franz law as its extreme expression, makes the experimental proof of the possibility of two thresholds in thermoelectric composites unlikely at present. Nevertheless, there are no bans on the existence of materials for which conditions (67)–(69) are met. A situation with double-threshold behavior of galvanomagnetic effects is more favorable.

III. GALVANOMAGNETIC EFFECTS

On application of the external magnetic field $\mathbf{H}$ to the isotropic conducting medium, the relation between current and field intensity assumes the form

$$\mathbf{j} = \hat{\sigma}(\mathbf{r})\mathbf{E}, \tag{70}$$

where

$$\hat{\sigma} = \begin{pmatrix} \sigma_x & \sigma_a & 0 \\ -\sigma_a & \sigma_x & 0 \\ 0 & 0 & \sigma_z \end{pmatrix}, \quad \mathbf{H} \| oz \tag{71}$$

is an antisymmetric tensor. The effective tensor $\hat{\sigma}_e$, similar to Eq. (2), interrelates volume averages of fields and currents,

$$\langle \mathbf{j} \rangle = \hat{\sigma}_e(\mathbf{H}) \langle \mathbf{E} \rangle. \tag{72}$$

In the simplest case, components of tensor $\hat{\sigma}$ are of the form

$$\sigma_x = \frac{\sigma}{1+\beta^2}, \quad \sigma_a = \frac{\sigma\beta}{1+\beta^2}, \quad \sigma_z = \sigma, \tag{73}$$

where σ is conductivity in the zero magnetic field, $\beta = \mu H / c$ is dimensionless magnetic field, μ is carrier mobility in the medium, and c is light velocity.

In the general three-dimensional case, for an arbitrary set of local kinetic coefficients of phases ($\hat{\sigma}_1$ and $\hat{\sigma}_2$ in the first and second phases, respectively), no isomorphism exists between the problems on galvanomagnetic properties and the one-flow problem—the problem of conductivity in the absence of a magnetic field. Therefore, to determine the concentration and field dependences of $\hat{\sigma}_e$, one should apply to some approximation. Here we shall use a generalized EMT approximation obtained in [11,12]. In this approximation, tensor $\hat{\sigma}_e$ is determined from the so-called self-consistent equation

$$(\hat{\sigma}_e - \hat{\sigma}_1)\hat{\gamma}(\hat{\sigma}_1, \hat{\sigma}_e)p + (\hat{\sigma}_e - \hat{\sigma}_2)\hat{\gamma}(\hat{\sigma}_2, \hat{\sigma}_e)(1-p) = 0, \tag{74}$$

where, as before, p is first phase concentration, and inverse to tensors $\hat{\gamma}(\hat{\sigma}_1, \hat{\sigma}_e) = \hat{\gamma}_1$ and $\hat{\gamma}(\hat{\sigma}_2, \hat{\sigma}_e) = \hat{\gamma}_2$, tensors $\hat{\Gamma}^1 = \hat{\gamma}_1^{-1}$, $\hat{\Gamma}^2 = \hat{\gamma}_2^{-1}$ are of the form

$$\hat{\Gamma}^i_{\alpha\beta} = \delta_{\alpha\beta} - \sum_\gamma n_{\alpha\gamma} \frac{(\hat{\sigma}_e - \hat{\sigma}_i)_{\gamma\beta}}{\sqrt{\sigma^e_{\alpha\alpha}\sigma^e_{\gamma\gamma}}}. \tag{75}$$

Here index $i=1,2$ is phase number and $n_{\alpha\beta}$ is a depolarization tensor [14], which for spherical inclusions is

$$n_{\alpha\beta} = \tfrac{1}{3}\delta_{\alpha\beta}. \tag{76}$$

Thus, for spherical inclusions and their isotropic arrangement, from Eq. (75) we find

$$\Gamma^i_{11} = \Gamma^i_{22} = 1 - \frac{1}{3}\frac{\sigma^e_x - \sigma^i_x}{\sigma^e_x}, \tag{77}$$

$$\Gamma^i_{12} = \Gamma^i_{21} = -\frac{1}{3}\frac{\sigma^e_a - \sigma^i_a}{\sigma^e_x}, \tag{78}$$

$$\Gamma^i_{33} = \Gamma^i_{22} = 1 - \frac{1}{3}\frac{\sigma^e_z - \sigma^i_z}{\sigma^e_z}, \tag{79}$$

$$\Gamma^i_{13} = \Gamma^i_{31} = \Gamma^i_{23} = \Gamma^i_{32} = 0, \tag{80}$$

where superscript $i=1,2$ is the phase number.

Finding the inverse to $\hat{\Gamma}$ tensor $\hat{\gamma}$ and substituting it into the self-consistent equations (74) yields a system of three equations to determine the effective conductivity,

$$\Omega^1_{11}p + \Omega^2_{11}(1-p) = 0,$$

$$\Omega^1_{12}p + \Omega^2_{12}(1-p) = 0,$$

$$\Omega^1_{33}p + \Omega^2_{33}(1-p) = 0, \tag{81}$$

where the superscript, as before, determines the phase, and the expressions for the components of tensor $\Omega^i_{\alpha\beta}$ are of the form

$$\Omega^i_{11} = (\sigma^e_x - \sigma^i_x)\frac{\Gamma^i_{11}}{(\Gamma^i_{11})^2 + (\Gamma^i_{12})^2} + (\sigma^e_a - \sigma^i_a)\frac{\Gamma^i_{12}}{(\Gamma^i_{11})^2 + (\Gamma^i_{12})^2},$$

$$\Omega^i_{12} = -(\sigma^e_x - \sigma^i_x)\frac{\Gamma^i_{12}}{(\Gamma^i_{11})^2 + (\Gamma^i_{12})^2} + (\sigma^e_a - \sigma^i_a)\frac{\Gamma^i_{11}}{(\Gamma^i_{11})^2 + (\Gamma^i_{12})^2},$$

$$\Omega^i_{33} = (\sigma^e_z - \sigma^i_z)\frac{1}{\Gamma^i_{33}}, \quad \Omega^i_{11} = \Omega^i_{22}, \quad \Omega^i_{21} = -\Omega^i_{12}. \tag{82}$$

The system of Eqs. (81) is nonlinear and its solution was obtained numerically. As an example, the values of tensor components $\hat{\sigma}_1$ and $\hat{\sigma}_2$ were chosen such that

$$\sigma^2_z \gg \sigma^1_z, \quad \sigma^2_x \ll \sigma^1_x. \tag{83}$$

In this case, conductivity "along" the magnetic field in the second phase is much higher in the first phase, therefore for σ^e_z one should anticipate a percolation transition close to $\tilde{p}_c$. For conductivity "across" the magnetic field, on the contrary, conductivity in the first phase is much higher in the second phase, and percolation behavior for σ^e_x is possible close to p_c. As to the nondiagonal component of σ^e_a, at appropriate values of local coefficients its behavior can be of percolation character close to both percolation thresholds. Selection of Eq. (83) is possible, since it follows from Eq. (73) on meeting the inequalities

$$\sigma_2 \gg \sigma_1, \quad \beta_2 \gg \beta_1. \tag{84}$$

Figure 4 shows concentration dependences of components of the effective tensor $\hat{\sigma}_e(\mathbf{H})$.

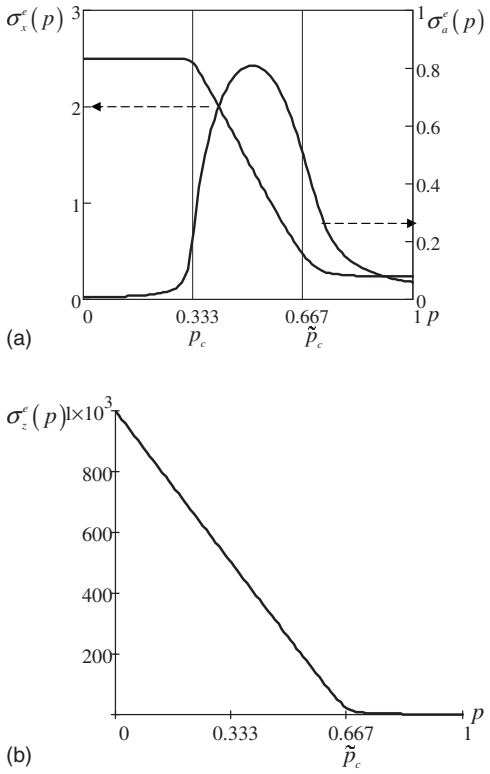

FIG. 4. Concentration dependences of components of effective tensor $\hat{\sigma}_e(\mathbf{H})$ are shown. (a) $\sigma^e_a(p)$; (b) $\sigma^e_z(p)$. The calculation was performed at $\beta_1=5$, $\beta_2=5\times10^4$ arb. units and $\sigma_1=1$, $\sigma_2=10^3$ arb. units.

IV. ON THE MODELS OF PERCOLATION STRUCTURES

In the description of kinetic effects in two-phase media close to the percolation threshold, in many cases it is convenient to use models of percolation structure (for example the Nodes-Links-Blobs model [15–21] or the hierarchical model [4,5,23,24]). In many cases, these models allow for the prediction of percolation behavior and/or an approximate calculation of critical exponents characterizing it. In the case of the simultaneous existence of double-threshold percolation behavior considered in this study, such models seemingly can give at least a qualitative description of the concentration and field dependences of effective kinetic coefficients. At present, however, it seems that for the cases in question, such a description is problematic. Indeed, for example, above the percolation threshold in all the models of percolation structure it is supposed that the basic structural element is a bridge—a combination of the so-called single connected bonds. Each of them, when broken, will stop current flow along the infinite cluster. The number of such series located on a semiconductor bridge (SCB), hence the bridge resistance, has a power dependence on the proximity to percolation threshold $\tau=(p-p_c)/p_c$. With a strong inhomogeneity of $\sigma_1 \gg \sigma_2$, an account of the second (small-conducting) phase introduces slight corrections. The second phase current distorts the first phase current only slightly. In the above case of double-threshold galvanomagnetic effects, Eq. (83), the situation is much more complicated. In the measurement of component σ^e_x, the average fields are also arranged along OX, and the bridge is largely located in the same direction. That is, its single connected bonds, arranged along OX, are much better current conductors than the second phase bonds arranged in the same direction. However, some SCBs (which meander more the closer they are to percolation threshold) are also arranged along OZ, and their conductivity (83) is much less compared to similar bonds of the second phase. Thus, it seems that the main elements of percolation struc-

ture (at least, in the case of galvanomagnetic phenomena) should include the bonds of both phases. Therefore, a "common" single-phase bridge consisting of single connected bonds cannot describe the double-threshold situation.

CONCLUSIONS

The cases in which two percolation thresholds of physical quantity can be observed in the same system have been considered above. In all these cases, it was supposed that percolation thresholds p_c and $\tilde{p}_c$ are far from each other. As is known, unlike critical exponents, the percolation threshold is not a universal value. It varies for different structures [3,22], for example in the problem of sites in the two-dimensional case for a square array $p_c=0.59$, for a honeycomb $p_c=0.7$, in the three-dimensional case with diamond structure $p_c=0.43$, in the problem of bonds for honeycomb $p_c=0.65(>1/2)$, and for the triangular $p_c=0.34(<1/2)$.

There can exist such an array or randomly inhomogeneous media when p_c and $\tilde{p}_c=1-p_c$ will draw together so much that critical areas close to these thresholds (i.e., an area where percolation behavior takes place) will be overlapped. In this case, it should be expected that standard percolation relations will occur no longer, and new types of concentration and field behavior of effective kinetic coefficients are possible.

A similar (see Fig. 3) two-threshold dependence for effective conductivity can be found in Ref. [25]. It should be noticed that two thresholds of percolation in this work are connected with a specially adopted arrangement of phases. In the randomly inhomogeneous grid, effective conductivity always has exactly one threshold of percolation. The same can be said about the medium when, in a homogeneous matrix, inclusions are scattered in a random way, for example spherically. But if inclusions have their own structure, i.e., an arrangement of phases is correlated, two thresholds of percolation can be observed in the medium [25].

The question regarding the value of p_c is a complex problem and should be considered for each concrete type of structure separately; see, for example, [26–31].

In our work, the case in which correlations in an arrangement of phases are absent is considered, and in the medium there are only two geometrical thresholds of percolation. This corresponds to the connectivity for the first and second phases. We consider such situations in which both thresholds influence the physical properties of the system.

[1] J. P. Clerc, G. Giraud, J. M. Laugier, and J. M. Luck, Adv. Phys. **39**, 191 (1990).
[2] D. J. Bergman and D. Stroud, Solid State Phys. **46**, 147 (1992).
[3] D. Stauffer and A. Aharony, *Introduction to Percolation Theory*, 2nd ed. (Taylor&Francis, London, 1992).
[4] A. E. Morozovskii and A. A. Snarskii, Zh. Eksp. Teor. Fiz. **95**, 1844 (1989) [Sov. Phys. JETP **68**, 1066 (1989)].
[5] A. A. Snarskii, A. E. Morozovsky, A. Kolek, and A. Kusy, Phys. Rev. E **53**, 5596 (1996).
[6] A. A. Snarskii and M. I. Zhenirovdkyy, e-print arXiv:cond-mat/07054031.
[7] J. P. Straley, J. Phys. D **14**, 2101 (1981).
[8] B. Ya. Balagurov, Zh. Eksp. Teor. Fiz. **85**, 568 (1983) [Sov. Phys. JETP **58**, 331 (1983)].
[9] D. A. G. Bruggeman, Ann. Phys. **25**, 645 (1936).
[10] R. Landauer, J. Appl. Phys. **23**, 779 (1952).
[11] D. Stroud, Phys. Rev. B **12**, 3368 (1975).
[12] D. J. Bergman and D. G. Stroud, Phys. Rev. B **62**, 6603 (2000).
[13] V. Halpern, J. Phys. C **16**, 2117 (1983).
[14] L. D. Landau, and E. M. Lifshitz, *Electrodynamics of Continuous Media, Course of Theoretical Physics* (Elsevier Butterworth-Heinemann, Oxford, 2004), Vol. 8.
[15] H. E. Stanley, J. Phys. A **19**, 211 (1977).
[16] A. Coniglio, Phys. Rev. Lett. **46**, 250 (1981).
[17] A. Coniglio, J. Phys. A **15**, 3829 (1982).
[18] R. Pike and H. E. Stanley, J. Phys. A **14**, 169 (1981).
[19] D. C. Wright, D. J. Bergman, and Y. Kantor, Phys. Rev. B **33**, 396 (1986).
[20] T. Ohtsuki and T. Keyes, J. Phys. A **11**, 559 (1984).
[21] A. S. Skal, Zh. Eksp. Teor. Fiz. **90**, 2057 (1986).
[22] B. I. Shklovskii and A. L. Efros, *Electronic Properties of Doped Semiconductors* (Nauka, Moscow, 1979).
[23] A. E. Morozovskii and A. A. Snarskii, Fiz. Tekh. Poluprovodn. (S.-Peterburg) **23**, 1220 (1989).
[24] A. A. Snarskii and A. E. Morozovsky, Int. J. Electron. **78**, 135 (1995).
[25] P. Sheng and R. V. Kohn, Phys. Rev. B **26**, 1331 (1982).
[26] J. B. Keller, J. Math. Phys. **5**, 548 (1964).
[27] A. M. Dykhne, Zh. Eksp. Teor. Fiz. **59**, 110 (1970) [Sov. Phys. JETP **32**, 63 (1970)].
[28] S. Torquato, *Random Heterogeneous Materials* (Springer-Verlag, New York, 2001).
[29] S. Kozlov, Russ. Math. Surveys **44**, 91 (1989).
[30] L. Berlyand and K. Golden, Phys. Rev. B **50**, 2114 (1994).
[31] K. M. Golden, in *Homogenization and Porous Media*, edited by U. Hornung (Springer-Verlag, New York, 1997), pp. 27–43.